Density stratification in an estuary with complex geometry: Driving processes and relationship to hypoxia on monthly to inter-annual timescales

Daniel L. Codiga[1]

Received 21 August 2012; revised 11 October 2012; accepted 19 October 2012; published 7 December 2012.

[1] The density field in Narragansett Bay (NB), a northeast U.S. estuary with complex geometry that suffers hypoxia, is described and related to driving factors using monthly means from time series observations at 9 sites during late spring to early fall 2001–2009. Stratification (deep-shallow density difference) is dominated by salinity and strongest (4–7 kg m^{-3} in late spring) near rivers in the north and east. Shallow horizontal density gradients are about 0.2 kg m^{-3} km^{-1}; deep densities have minor spatial and seasonal variations. Geographic structure in density, and its inter-annual anomalies, is weaker than expected based on the complex geometry and large size relative to the internal deformation radius. Inter-annual variability is primarily driven by river flow and weakly influenced by winds, contrasting nearby systems (Chesapeake Bay, Long Island Sound), likely due to reduced fetch and/or unfavorable alignment with prevailing winds. Stratification response to river flow follows 2/3 power scaling despite that the theory omits important NB attributes (complex geometry, depth-varying horizontal gradients). Contrasting other systems (Delaware Bay, San Francisco Bay), horizontal gradients are at least as responsive to river forcing as theoretical 1/3 power scaling; depth-dependent horizontal gradients or finite basin constraint of intrusion length may be responsible. Bay-wide inter-annual variations in seasonal hypoxia correlate with late spring stratification, though stratification peaks in the north and east with hypoxia most severe in the north and west. Long-term response of stratification, and thus its role in hypoxia, to climate-driven increases in river flow and temperatures will be dominated by the former.

Citation: Codiga, D. L. (2012), Density stratification in an estuary with complex geometry: Driving processes and relationship to hypoxia on monthly to inter-annual timescales, *J. Geophys. Res.*, *117*, C12004, doi:10.1029/2012JC008473.

1. Introduction

[2] Estuaries are important for many reasons, including high biological productivity. They are numerous and the diversity of coastline and bathymetric configurations is enormous. A fundamental system characteristic is the density field, including stratification (the vertical gradient) and the structure of the horizontal gradient from the oceanic limit toward the freshwater limit. Density distributions closely control circulation and vertical mixing, and play a role in development of hypoxia, a major threat to the health of estuarine ecosystems. Density responds to a number of driving factors including freshwater inputs, the surface heat flux, wind-forcing, and tidal mixing conditions. Density structure, and its relationship to driving factors, varies strongly from estuary to estuary and within individual systems. Improved understanding is needed.

[3] This paper uses observations to investigate dynamics of density structure in Narragansett Bay (NB; Figure 1) and its connection to hypoxia. Interpretations are made in the context of comparisons to other estuaries and theoretical expectations, and implications for climate change are explored. NB is a temperate northeastern U.S. estuary representative of relatively shallow systems of moderate size with weak river forcing, and is distinguished by its complicated passageway and embayment geometry. The focus here is on variability at monthly and longer timescales, with emphasis on the seasonal progression and inter-annual variability. Variability on shorter timescales can be energetic, for example due to weather-band wind fluctuations up to several days long, and spring-neap tidal variations, but will be addressed elsewhere.

[4] The complex passageway/embayment geometry makes NB a good site to investigate the extent to which coastline configuration affects the response of the density field to forcing. In NB estimates of the Kelvin number [e.g., *Garvine*, 1995], or ratio between the width of the bay (as well as most of its individual passages) and the internal radius of deformation, are at least of order one and imply that background rotation is important. This supports the hypothesis,

[1]Graduate School of Oceanography, University of Rhode Island, Narragansett, Rhode Island, USA.

Corresponding author: D. L. Codiga, Graduate School of Oceanography, University of Rhode Island, Narragansett, RI 02882, USA. (d.codiga@gso.uri.edu)

©2012. American Geophysical Union. All Rights Reserved.
0148-0227/12/2012JC008473

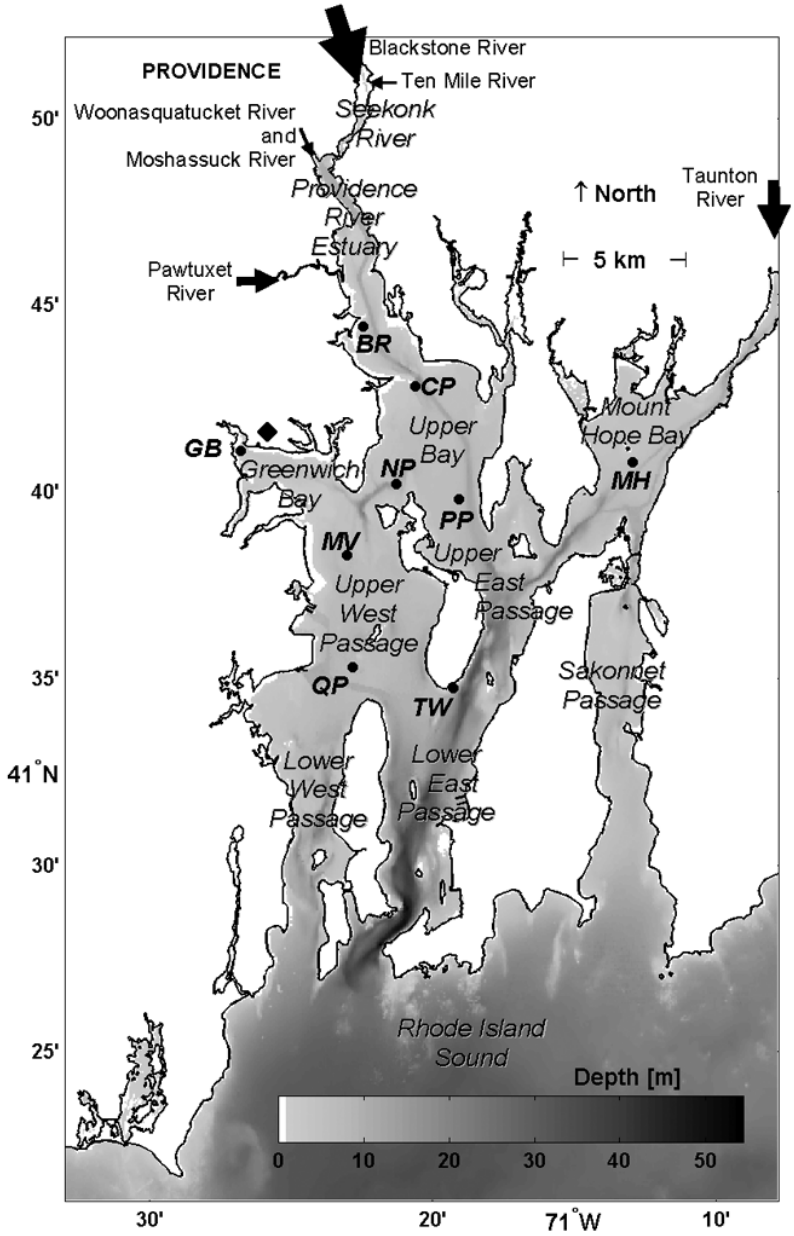

Figure 1. Narragansett Bay geography, bathymetry, place names, rivers, and sampling stations (abbreviations in Tables 1–4). River arrow size is proportional to annual-mean flow. Diamond at northern edge of Greenwich Bay shows location of N.A.R.R. grid point for winds.

investigated here, that there will be substantial geographic variability in the density structure in NB, and in its response to forcing.

[5] NB is one of several northeast U.S. estuaries and in two nearby systems inter-annual variability in stratification and hypoxia are sensitive to wind variations. In both Chesapeake Bay (CB) [*Scully*, 2010] and Long Island Sound (LIS) [*Wilson et al.*, 2008], climate-driven shifts in summer winds alter vertical mixing conditions and explain more inter-annual variability in hypoxia than nutrient loading does. An important question, thus taken up here, is whether inter-annual variability of stratification and hypoxia in NB are similarly sensitive to wind variations.

[6] Theory for non-rotating partially stratified estuaries with simple channel geometry provides scaling relations, that are independent of mixing parameterization details so potentially of broad applicability, for the response of the density field to river flow [e.g., *Hetland and Geyer*, 2004; *MacCready and Geyer*, 2010]. At timescales longer than the adjustment time, in systems forced mainly by river flow and having exchange-dominated residual circulation as in NB, the stratification and the along-axis density gradient scale as the 2/3 and 1/3 power, respectively, of river flow. These relations are used here to put observed NB responses, at timescales longer than its estimated adjustment time as appropriate for comparison to the scaling, in the context of dynamics in other systems such as Delaware Bay and San Francisco (SF) Bay.

[7] Hypoxia is negatively impacting NB [e.g., *Altieri and Witman*, 2006; *Codiga et al.*, 2009; *Deacutis*, 2008], has led to costly sewage treatment modifications presently being implemented [e.g., *Rhode Island Department of Environmental Management* (*RIDEM*), 2005], and has been shown to be linked to stratification [*Bergondo et al.*, 2005; *Codiga et al.*, 2009; *Deacutis et al.*, 2006; *Melrose et al.*, 2007]. However, questions remain about the relationship between stratification and hypoxia, which motivate the present analysis. For example, are geographic patterns in hypoxia and stratification similar, as would be expected under the paradigm of one-dimensional vertical dynamics (deep hypoxia enhanced when stratification suppresses mixing)?

[8] NB consists of three main north-south oriented passages (West Passage, East Passage, and Sakonnet Passage) that exchange with each other at multiple locations, and with several embayments, some of which have river inputs (Figure 1). Depths are typically less than 10 m but reach 40–50 m in the lower East Passage. Sakonnet Passage is isolated from the rest of the system by a narrow constriction at its northern end, and has not been sampled so is not treated here. River inputs are concentrated in the north, particularly entering the Providence River Estuary (PRE). The average tidal range is about 1–1.5 m and tidal currents are about 10–50 cm/s with peak values near constrictions [e.g., *Spaulding and Swanson*, 2008]. Current variability on weather band timescales is energetic [e.g., *Weisberg and Sturges*, 1976]. Non-tidal residual circulation was deduced to consist of a two-layer estuarine exchange flow, in which coastal waters are delivered to the system primarily through the lower East Passage from Rhode Island Sound (RIS) to the south, from early hydrographic measurements [*Fish*, 1953; *Hicks*, 1959]. Direct measurements of the residual circulation (reviewed by *Spaulding and Swanson* [2008]) are limited but do not contradict this concept, and realistic modern numerical simulations [*Rogers*, 2008] generally support it. Estimated residence times at the bay-wide scale range from about 10 to 40 days [*Pilson*, 1985] while the flushing time of the PRE has been estimated at about 1–8 days [*Asselin and Spaulding*, 1993].

[9] The density field in NB has received relatively little attention. Early work [*Fish*, 1953; *Hicks*, 1959] identified large-scale horizontal and vertical patterns of temperature and salinity from a few vessel-based hydrographic surveys, and *Kremer and Nixon* [1978] presented an annual cycle of surveys, but neither density nor stratification were examined. Modern conductivity-temperature-depth (CTD) surveys at ~50+ stations with good spatial coverage of the northern half of the bay document significant stratification, with peak sigma-t differences on short timescales reaching 10–15 kg/m^3 in and near the PRE and up to 5 kg/m^3 at mid-estuary locations [e.g., *Deacutis et al.*, 2006]. Similar stratification is seen in vertical-axial structure of density as measured along the channel in the passages using a towed undulating CTD on once-monthly cruises [*Berman*, 2008]. Early time series observations collected by buoys have demonstrated strong variability in densities on timescales from hours to weeks [*Bergondo et al.*, 2005]. Here, records from 2001 to 2009 sampled during the late spring to early fall period are treated, from nine sites spanning the northern half of the bay (Figure 1); the monthly mean stratification based on frequently sampled time series is used because, unlike vessel-based surveys, it eliminates aliasing of shorter-timescale variability.

2. Observations and Methods

2.1. Temperature, Salinity, and Oxygen Observations

[10] Temperature, salinity, and dissolved oxygen (DO) observations of the Narragansett Bay Fixed Site Monitoring Network [*Bergondo*, 2004; *Narragansett Bay Fixed-Site Monitoring Network* (*NBFSMN*), 2004, 2005, 2006, 2007b, 2008, 2009; *Stoffel*, 2003] are used. *NBFSMN* [2007a] stations (Figure 1) are mostly buoys with a few pier-based sites, deployed May to October. Each station treated has sensors at two depths, nominally 1 m deep and 0.5 m above the seafloor (sensor depths and seafloor depths are listed in the headings of each inset frame in Figures 3–5), and collects 15-min resolution time series. *NBFSMN* [2006], *RIDEM* [2007], and Table 1 of *Codiga et al.* [2009] provide additional information. Practical Salinity Scale (PSS) units are used for salinity.

[11] For convenience the nine stations (Figure 1) are organized in four groups. The Upper Bay group (UB) includes three stations in the PRE and the Upper Bay, namely Bullocks Reach (BR), Conimicut Point (CP), and North Prudence (NP). The West Passage (WP) group includes the Mount View (MV) and Quonset Point (QP) stations. The East Passage group includes the Poppasquash Point (PP) and Prudence Island T-Wharf (TW) stations. The Embayments group (EM) includes Greenwich Bay (GB) and Mount Hope Bay (MH) stations.

[12] Throughout this analysis "stratification" refers to the difference in density (sigma-t) between the deep and shallow sensors. When non-uniform, vertical profiles of sigma-t [see, e.g., *Deacutis et al.*, 2006] are most often characterized by a pycnocline that is centered at least 2 m deep, spans a depth range of nominally 1–2 m, and separates two relatively uniform layers; other profile shapes, such as more nearly linear increases over a large fraction of the water column, occur but are far less common. NBFSMN shallow and deep sensors nearly always straddle the pycnocline, so their density difference characterizes that between the above- and below-pycnocline layers; this holds regardless of the pycnocline depth as long as it is deeper than the shallow sensor. The buoyancy frequency was not found to be a useful metric; its computation includes normalizing density differences by the depth difference between the two sensors, which increases at deeper sites (see, e.g., headings of inset frames in Figure 3), so yields lower buoyancy frequencies there, even in the idealized case of a horizontally uniform two-layer constant-depth pycnocline, and thus confounds interpretation of geographic differences. Stated differently, given two-depth sampling the density difference between deep and shallow sensors, while recognized to be insensitive to changes in the pycnocline depth, is nonetheless the more pertinent metric because it is more representative of the net across-pycnocline density change than buoyancy frequency based on the two sensors.

[13] All available 2001–2009 NBFSMN observations from May 15 to Oct 15 are used (Tables 1–4). Five one-month intervals (e.g., from May 15 to Jun 15, Jun 15 to Jul 15, etc) are used to examine the seasonal progression from spring through summer to early fall. The average across the entire five-month interval is referred to as the 5-month mean and used to characterize the mean conditions, from late spring to early fall, for

Table 1. Sampling of Density Stratification, Providence River Estuary and Upper Bay Stations[a]

	MJ	JJ	JA	AS	SO	MO
BR						
2001	100%	100%	100%	100%	100%	100%
2002	27%	69%	100%	92%	100%	77%
2003	78%	100%	76%	68%	75%	79%
2004	92%	100%	100%	100%	100%	98%
2005	46%	100%	100%	100%	100%	89%
2006	33%	92%	68%	100%	70%	73%
2007	68%	46%	52%	78%	13%	52%
2008	100%	100%	100%	100%	82%	96%
2009	100%	100%	100%	100%	100%	100%
#Yrs > 55%	6	8	8	9	8	8
CP						
2003	27%	100%	57%	100%	34%	64%
2005	48%	36%	89%	100%	100%	75%
2006	2%	100%	100%	100%	100%	80%
2007	68%	100%	100%	100%	100%	94%
2008	81%	100%	100%	100%	100%	96%
2009	24%	100%	100%	100%	100%	85%
#Yrs > 55%	2	5	6	6	5	6
NP						
2001		48%	100%	100%	100%	69%
2002	5%	100%	100%	100%	100%	81%
2003	30%	100%	100%	97%	54%	76%
2004	40%	100%	100%	100%	95%	87%
2005	73%	69%	100%	100%	90%	86%
2006	86%	28%	65%	86%	52%	64%
2007	65%	30%	95%	100%	100%	78%
2008	17%	100%	100%	100%	64%	76%
2009	62%	100%	65%	62%	98%	77%
#Yrs > 55%	4	6	9	9	7	9

[a]Percent of time density stratification was sampled (both shallow and deep temperature and salinity sensors collected data meeting quality control standards) at Bullocks Reach "BR," Conimicut Point "CP," and North Prudence "NP." Five one-month intervals (MJ = May 15 to Jun 15, JJ = Jun 15 to Jul 15, JA = Jul 15 to Aug 15, AS = Aug 15 to Sep 15, SO = Sep 15 to Oct 15), and the interval spanning all five months (MO, May 15 to October 15), are shown. The bottom row for each station shows number of years with percent coverage greater than 55%.

a given year. Some stations (BR, NP) were sampled starting in 2001 and have 8 or 9 years during which temporal coverage reached at least 55% from May to Oct (bottom row of Tables 1–4 for each station). Other stations have been maintained only during more recent years so have fewer years of sampling, typically 5–7, with a minimum of 4 years at QP.

Table 2. Sampling of Density Stratification, West Passage Stations[a]

	MJ	JJ	JA	AS	SO	MO
MV						
2004		49%	100%	86%	95%	66%
2005	46%	46%	46%	100%	100%	68%
2006	94%	100%	100%	100%	93%	97%
2007	65%	69%	63%	33%	85%	63%
2008	68%	100%	100%	100%	100%	94%
2009	59%	77%	100%	71%	97%	81%
#Yrs > 55%	4	4	5	5	6	6
QP						
2005			52%	76%		26%
2006	89%	100%	52%	35%	26%	60%
2007		33%	87%	100%	100%	64%
2008	84%	100%	100%	100%	100%	97%
2009	59%	97%	60%	87%	100%	80%
#Yrs > 55%	3	3	3	4	3	4

[a]As Table 1 but for Mount View (MV) and Quonset Point (QP) stations.

Table 3. Sampling of Density Stratification, East Passage Stations[a]

	MJ	JJ	JA	AS	SO	MO
PP						
2004		25%	100%	100%	93%	64%
2005			37%	98%	33%	34%
2006	94%	100%	100%	100%	100%	99%
2007	65%	100%	92%	100%	100%	91%
2008	84%	100%	79%	100%	100%	93%
2009	59%	82%	100%	100%	100%	88%
#Yrs > 55%	4	4	5	6	5	5
TW						
2003	100%	100%	59%	52%	100%	82%
2004	46%	100%	100%	100%	100%	89%
2005	100%	51%	100%	100%	100%	90%
2006	49%	100%	100%	87%	100%	87%
2007	100%	100%	60%	46%	97%	80%
2008	100%	100%	84%	100%	100%	97%
2009	100%	100%	90%	100%	87%	95%
#Yrs > 55%	5	6	7	5	7	7

[a]As Table 1 but for Poppasquash Point (PP) and Prudence Island T-Wharf (TW) stations.

[14] The representativeness of means and standard deviations at stations with the fewest years sampling (QP: 4 years, 2006–2009; PP: 5 years, 2004 and 2006–2009; and MH: 5 years, 2005–2009) was tested as follows, using the stations with the highest number of years sampled (NP: 9 years, 2001–2009; BR: 8 years, 2001–2009 except 2007). The multiyear mean and standard deviation of inter-annual variability in the shallow and deep 5-month mean densities were computed at NP and BR using all available years, and compared to the results when instead computed using the subset of years sampled at QP, PP, and MH. Changes to shallow means, as a percent of the standard deviation computed with all available years, ranged from −22% to +5% when computed using subsets of years; for deep means the changes ranged from −36% to +46%. Changes to shallow standard deviations, also as a percent of the standard deviation computed with all available years, ranged from −17% to 2%; for deep standard deviations the range was −44% to 21%. These ranges of variation, and asymmetries between positive and negative changes, are sufficiently small to indicate that

Table 4. Sampling of Density Stratification, Embayment Stations[a]

	MJ	JJ	JA	AS	SO	MO
GB						
2003		64%	100%	100%	52%	63%
2004	62%	100%	98%	52%	100%	82%
2005	22%	79%	100%	100%	97%	79%
2006	95%	100%	95%	100%	100%	98%
2007	38%	100%	95%	76%	61%	74%
2008	70%	74%	100%	100%	100%	89%
2009	79%	66%	100%	100%	100%	89%
#Yrs > 55%	4	7	7	6	6	7
MH						
2005		36%	100%	100%	69%	61%
2006	90%	100%	100%	100%	100%	98%
2007	65%	64%	100%	100%	100%	86%
2008	19%	100%	100%	100%	100%	84%
2009	40%	100%	100%	100%	97%	87%
#Yrs > 55%	2	4	5	5	5	5

[a]As Table 1 but for Greenwich Bay (GB) and Mount Hope Bay (MH) stations.

results from stations with fewer sampled years are not unrepresentative.

[15] The DO observations are used to compute a seasonal hypoxia index as follows. Hypoxic events and their deficit-duration (mg l^{-1} day) relative to threshold 2.9 mg O_2 l^{-1} are determined by the "moving window trigger" method [*Codiga*, 2008] based on the 15-min resolution records and using trigger duration of 9 h and minimum event duration of 1 day [*Codiga et al.*, 2009]. The season-cumulative deficit-duration (mg l^{-1} day) is normalized by the number of sampled days that year to yield the seasonal hypoxia index (mg l^{-1}). An average across data available from stations BR, CP, NP, and MV is representative of bay-wide hypoxia, because they are located in the relatively deep portions of the northern and western portions of the bay, where hypoxia has been shown to be most prevalent [*Codiga et al.*, 2009].

2.2. Driving Factors

[16] River flow data are U.S. Geological Survey daily values at the six largest sources (Figure 1): the Blackstone, Taunton, Pawtuxet, Ten Mile, Woonasquatucket, and Moshassuk Rivers, in order of decreasing average volume. Response to river forcing is investigated using the Taunton for MH and the sum over the other five rivers for all other stations.

[17] The raw net air-sea heat flux is computed using the 3-h resolution North American Regional Reanalysis (NARR), a data-assimilative operational meteorological model product with spatial resolution of about 40 km in this region [*Mesinger et al.*, 2006]. Values from 2001 to 2009 were used from the over-water grid point nearest Narragansett Bay, in north-central Rhode Island Sound (41° 18.408′ 71° 15.324′) about 5 km south of the bottom of Figure 1. Net heat flux (positive from atmosphere to ocean) was computed as the summed downward shortwave and longwave radiative fluxes less the corresponding upward fluxes, plus the sensible and latent heat fluxes.

[18] Raw winds are from NARR during 2001–2009 at the over-land grid point nearest NB, which is just north of Greenwich Bay (Figure 1). They compare well with local wind records (e.g., Narragansett Bay Physical Oceanographic Real Time System, tidesandcurrents.noaa.gov) which are not used due to temporal coverage gaps. Directional constancy is 100*(vector-average wind magnitude)/(mean wind speed).

2.3. Analysis Methods

[19] Raw time series of NBFSMN observations other than oxygen (for which analysis is described above at the end of section 2.1), and auxiliary parameters of driving factors, are low-pass filtered with a 25-h half-width triangle-weight filter to suppress tidal variability, then subsampled to 12-h resolution, and used to compute monthly means. Inter-annual variability is characterized by the standard deviation of the monthly mean values available during 2001–2009. Deviations from the seasonal progression, used to investigate inter-annual variability, consist of monthly mean values less the multiyear average of monthly means for that month.

[20] The percent contribution of salinity to vertical density differences is computed as

$$100 * (\sigma_t[S(dp), \langle T\rangle] - \sigma_t[S(sh), \langle T\rangle])/(\sigma_t[S(dp), T(dp)] - \sigma_t[S(sh), T(sh)]),$$

where σ_t[S, T] denotes the equation of state for sigma-t, S(dp) and S(sh) are the deep and shallow salinities, and $\langle T\rangle$ is the mean of the deep and shallow temperatures T(dp) and T(sh). A value greater than 100 can occur when the deep measurement is warmer so temperature is destabilizing; this occurred (104%) only at one site, GB, during one of the five one-month averaging intervals (Sep 15–Oct 15).

[21] In treating horizontal structure (Section 3.3) each station is assigned a "down-estuary distance" (as opposed to the linear North-South distance) to represent its distance, in the along-passageway direction, toward the southern end of the estuary. The origin is taken to be the northernmost station (BR) and the bay is divided (Figure 1) in to western and eastern passageway topologies, both sharing the two northernmost stations (BR and CP). In the west the sequence is BR, CP, NP, MV and QP; in the east it is BR, CP, PP, and TW. The down-estuary distance is the cumulative unadjusted distances between stations. For example, the down-estuary distance of NP (8.8 km) is the sum of the actual distance between BR and CP (3.9 km) and the actual distance between CP and NP (4.9 km). The two embayment stations GB and MH, each treated independently, are assigned down-estuary distances based on their proximity to stations in each of the east and west topologies; specifically, GB has a down-estuary distance between those of NP and MV, and MH has a down-estuary distance between those of PP and TW. Though crude, down-estuary distances defined in this way are nonetheless sufficient for the gross characterizations made of horizontal structure and gradients. Horizontal gradients between deep sensors are based on differences between the values measured by the sensors regardless of their depths, with the result that for station pairs with deep sensors at different depths, the "horizontal gradient" reflects both the horizontal difference as well as the difference in depth. The latter component contributes little to the total because, as explained above, deep sensors lie in a relatively homogenous layer.

[22] To investigate driving factors for inter-annual variability in stratification, Kendall's τ correlations were computed between monthly stratification deviations and similarly defined deviations (from multiyear means, 2001–2009) of monthly mean driving factors: river runoff, surface heat flux, and wind parameters. No lags were included because the longest estimated flushing time for the estuary (40 days [*Pilson*, 1985]) is closer to one month than two months and the calculation is based on monthly mean quantities. The wind parameters used were the wind speed and directional constancy, and wind components directed toward the N, NNE, NE, ENE, E, ESE, SE, and SSE. Wind speed is a proxy for local wind-driven mixing; results using wind speed squared (representative of wind stress) or wind speed cubed (representative of energy available for mixing [e.g., *Niiler and Kraus*, 1977]) do not lead to substantially different conclusions. Wind components in eight directions are proxies for local advective and straining influences, which are expected to depend on the orientation of the wind relative to the passageway. Inclusion of eight wind directions covers 16 points of the compass because the correlation results will be the same, except for the sign of τ, for oppositely directed winds.

[23] A least squares fit of stratification $\Delta\rho$ (deep minus shallow density, kg m^{-3}) to the nonlinear model kQ^{α}, a power law dependence on river flow Q (m^3 s^{-1}), determines values for k and unitless α at each station by the Levenberg-Marquardt method [e.g., *Seber and Wild*, 2003] using Matlab

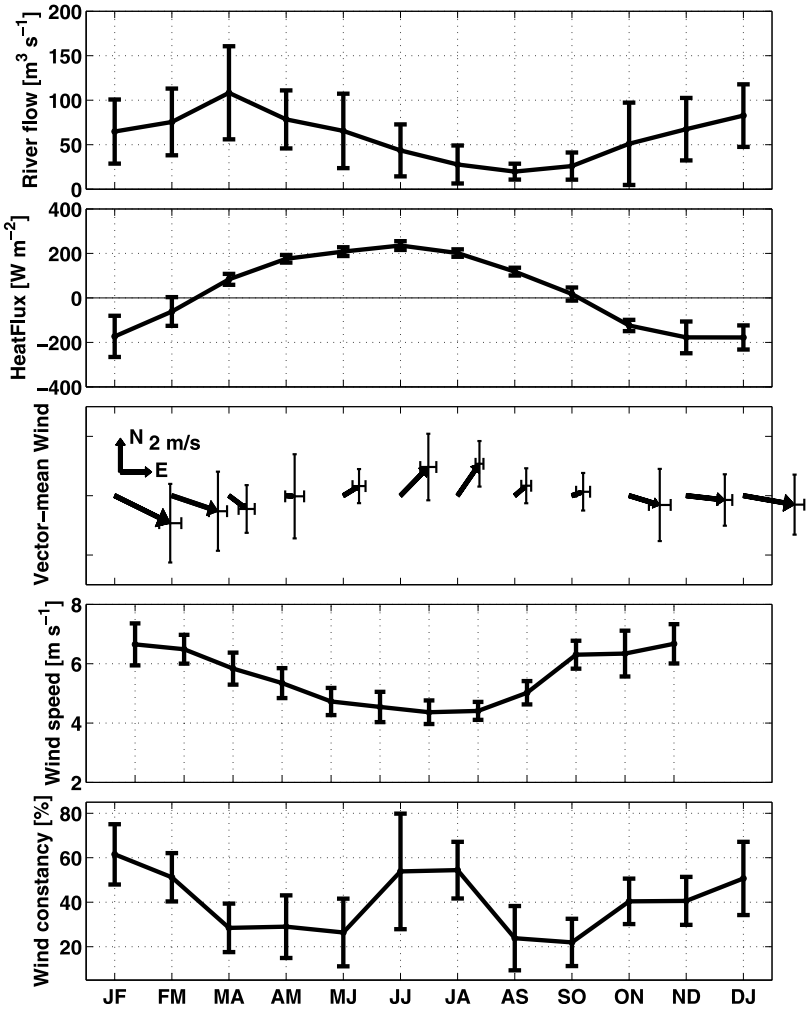

Figure 2. Seasonal cycle of driving factors. Monthly means of low-passed time series, from 2001 to 2009. Error bars depict standard deviation of inter-annual variations in monthly means. Horizontal axis labels monthly intervals (JF for 15 January to 15 February, FM for 15 February to 15 March, etc.).

function *nlinfit()*. Confidence intervals on α, and on outputs of the nonlinear model, are estimated by the asymptotic normal distribution method [e.g., *Bates and Watts*, 1988] using Matlab functions *nlparci()* and *nlpredci()*.

[24] The same power law model and analysis used for stratification is also applied to horizontal density gradients. The horizontal gradient between two stations is calculated as the difference of the mean shallow and deep density values, weighted in proportion to the shallow and deep layer thicknesses, and using along-estuary distances defined as described above. The shallow layer thickness is taken to be 2.5 m and constant bay-wide, a representative choice based on CTD casts [e.g., *Deacutis et al.*, 2006]. The BR-NP, BR-QP, and BR-TW station pairs are used as representative of horizontal gradients along the PRE, the upper West Passage, and the upper East Passage respectively.

3. Results

3.1. Forcing: Rivers, Air-Sea Heat Flux, Winds

[25] Monthly means and their standard deviations over 2001–2009 (Figure 2) depict the annual cycles of the main driving factors. River inputs peak in spring, are minimal in late summer, and have substantial inter-annual variability; underlying the monthly mean values are conditions typified by the highest number of storm-related runoff events in the spring, a lesser amount in fall, and the fewest in summer (for more detailed information see *Ries* [1990]). Net air-sea heat flux is positive from about March through the end of September, with modest inter-annual variability except during the winter months not considered here. Winds transition from wintertime conditions of higher speeds and an east-southeastward mean direction to lower speeds and a generally northeastward mean direction in summer, with substantial inter-annual variability in all months. Wind directional constancy is highest in winter and mid-summer, lowest in spring and early fall, and has significant inter-annual variability.

3.2. Temperature, Salinity, Density: Seasonal Progression and Geographic Structure

[26] The geographic structure and seasonal progression of shallow and deep temperature, salinity, and density (sigma-t) fields, together with their vertical differences, are presented in Figures 3, 4, and 5 respectively. Temperatures (Figure 3) are relatively uniform geographically and follow the expected

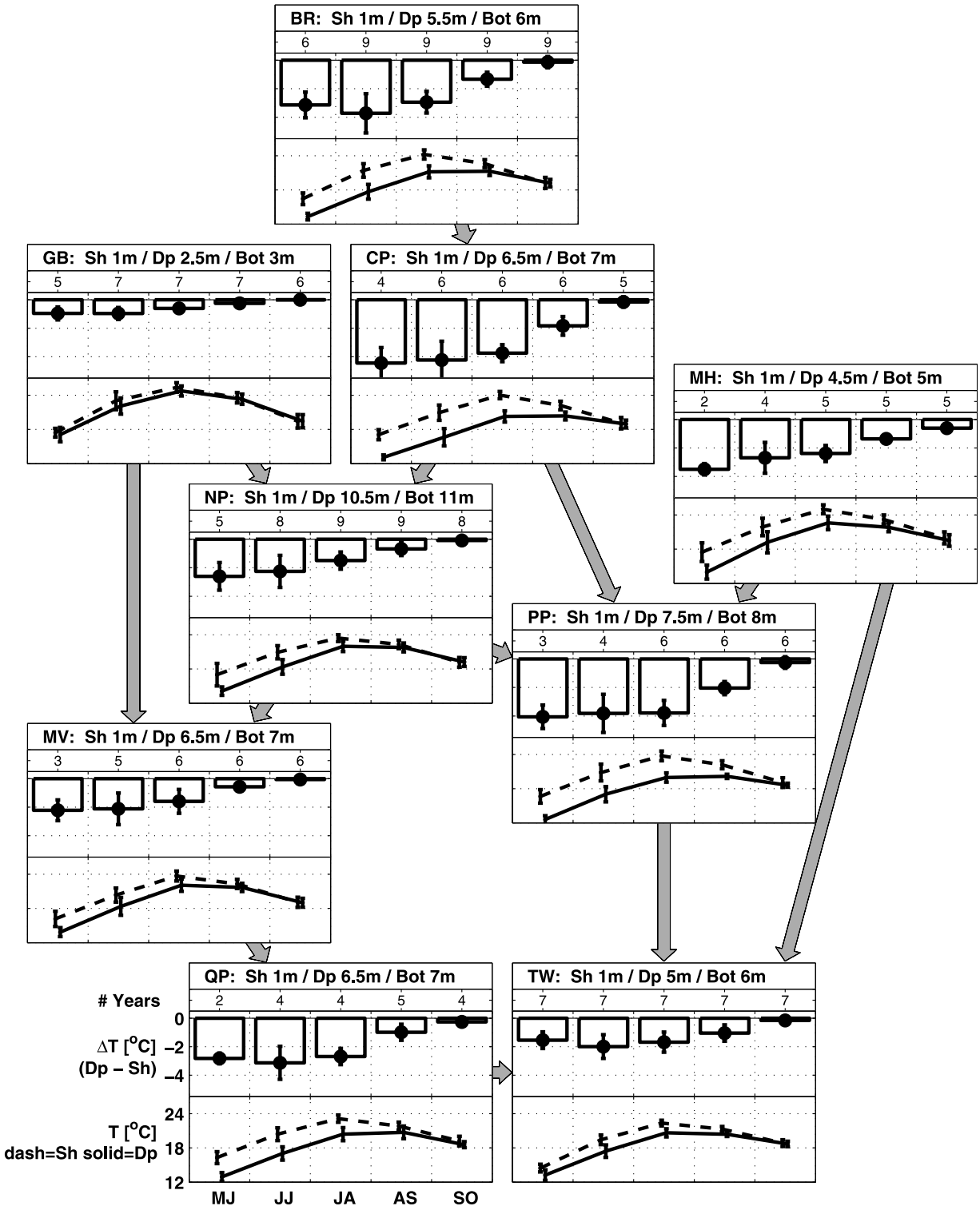

Figure 3. Seasonal progression of temperature and vertical difference of temperature. Curves and barplots: multiyear averages; error bars: inter-annual standard deviations. Frames arranged to correspond with station geographic locations. Legends at bottom left; frame headings show station abbreviation, depth of the shallow (Sh) and deep (Dp) sensors, and seafloor depth (Bot). The 5 one-month intervals (e.g., MJ = May 15 to Jun 15, see Table 1) span late spring to fall. Upper plot in each frame shows vertical difference (deep – shallow) as bar graph, with the number of years used (bottom rows of Tables 1–4) shown above each bar. Bottom plot in each frame shows shallow (dashed) and deep (solid) values, with small right-left offsets for clarity to avoid overlap of error bars. Wide gray background arrows point toward the nearest neighboring station in the direction toward the primary source of oceanic water entering the bay, the southern end of East Passage.

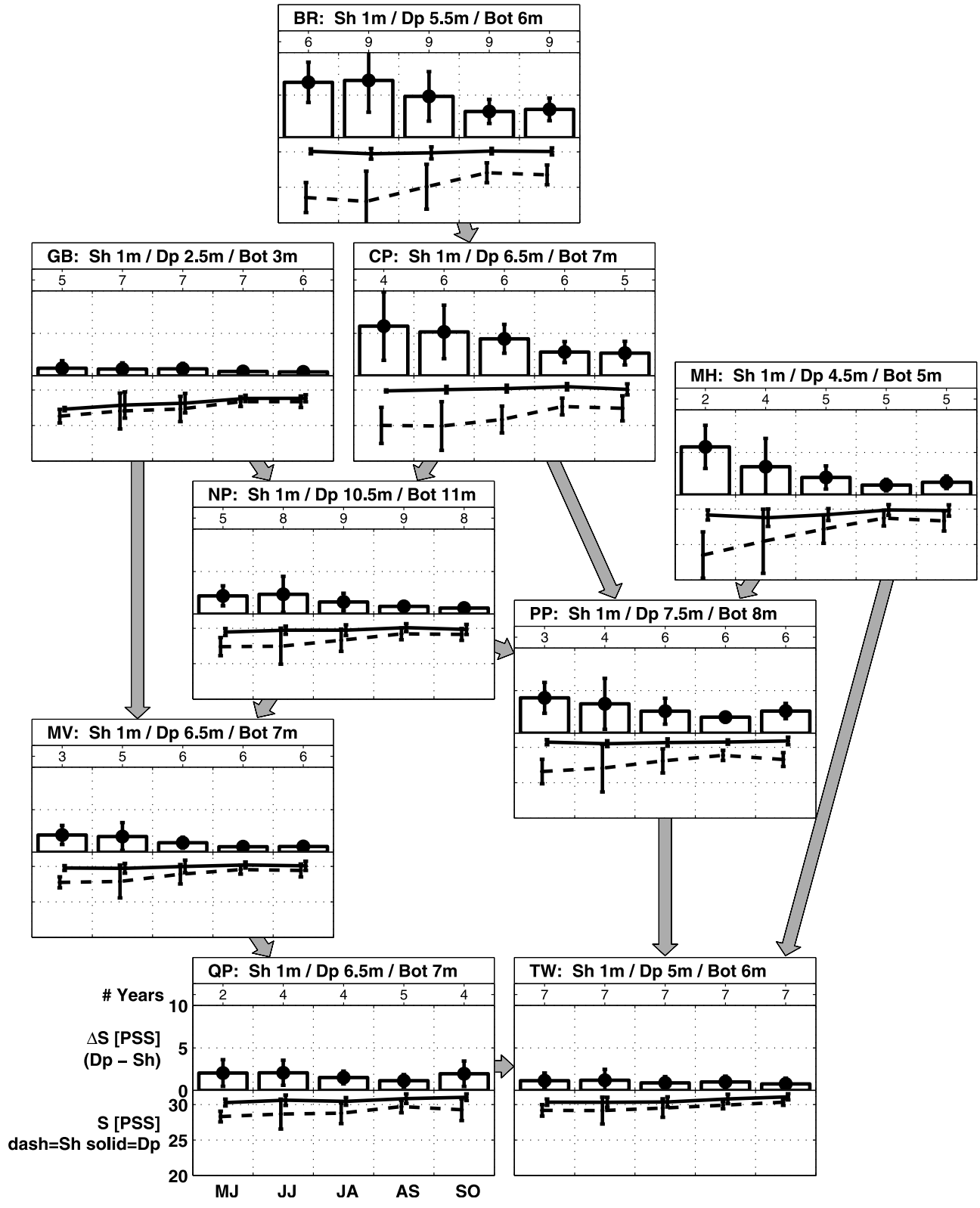

Figure 4. Seasonal progression of salinity and vertical salinity difference, shown as in Figure 3.

seasonal cycle, an indication that the air-sea heat flux is the dominant influence. Deep values are generally lower such that temperature acts to strengthen density stratification. In general the summer peak near the surface is a few degrees higher, and occurs roughly a month earlier (JA instead of AS), as compared to that at depth. Vertical differences in temperature reach 3–5 C in late spring and early summer (MJ or JJ) and are gone by early fall (SO). Geographic structure in the vertical differences is modest, with the largest values, by a small margin, at BR, CP, and PP.

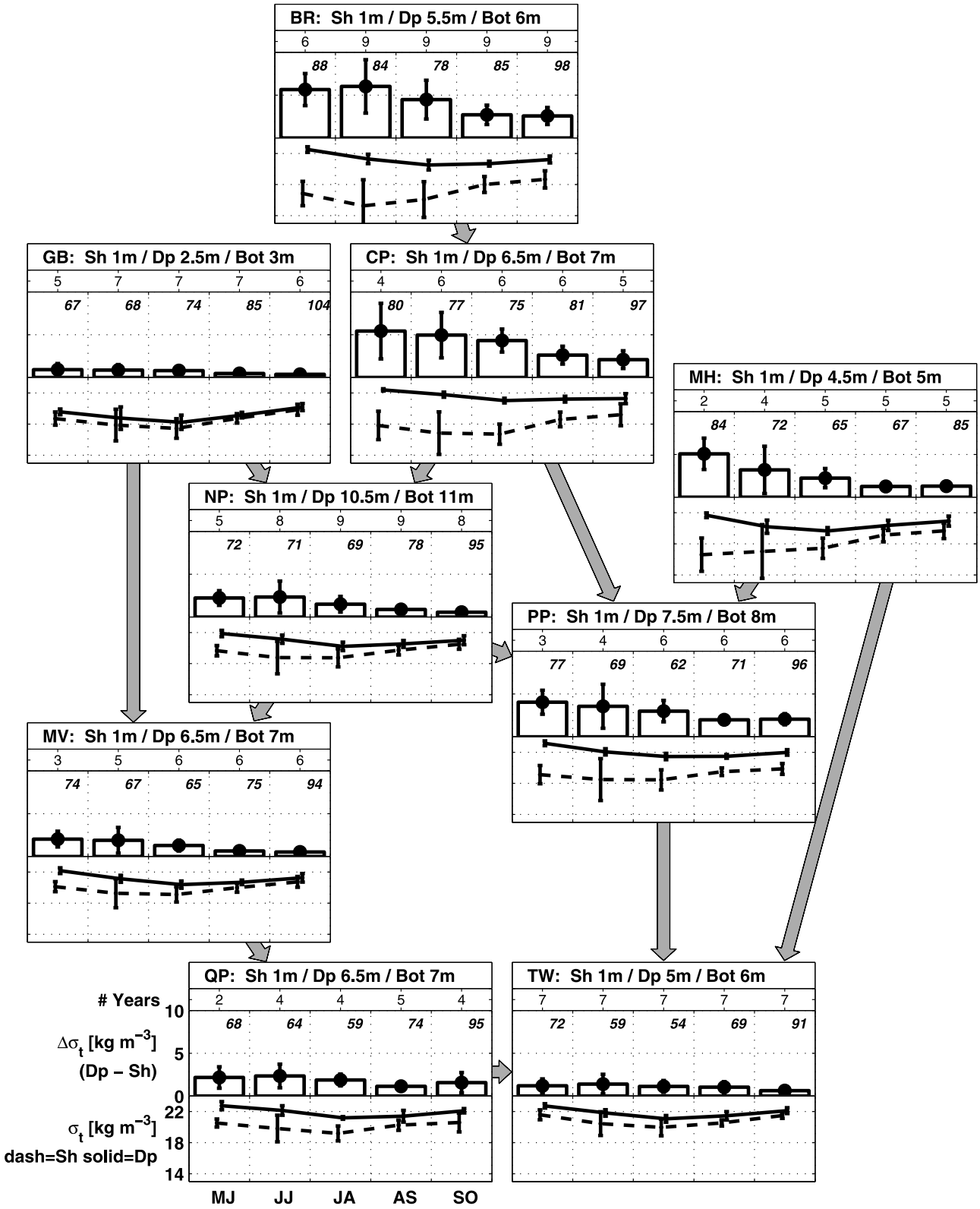

Figure 5. Seasonal progression of density (sigma-t) and stratification (vertical density difference), shown as in Figure 3. The percent of the vertical density difference due to salinity, relative to the total vertical density difference, is shown in bold above the bars in the bar graphs.

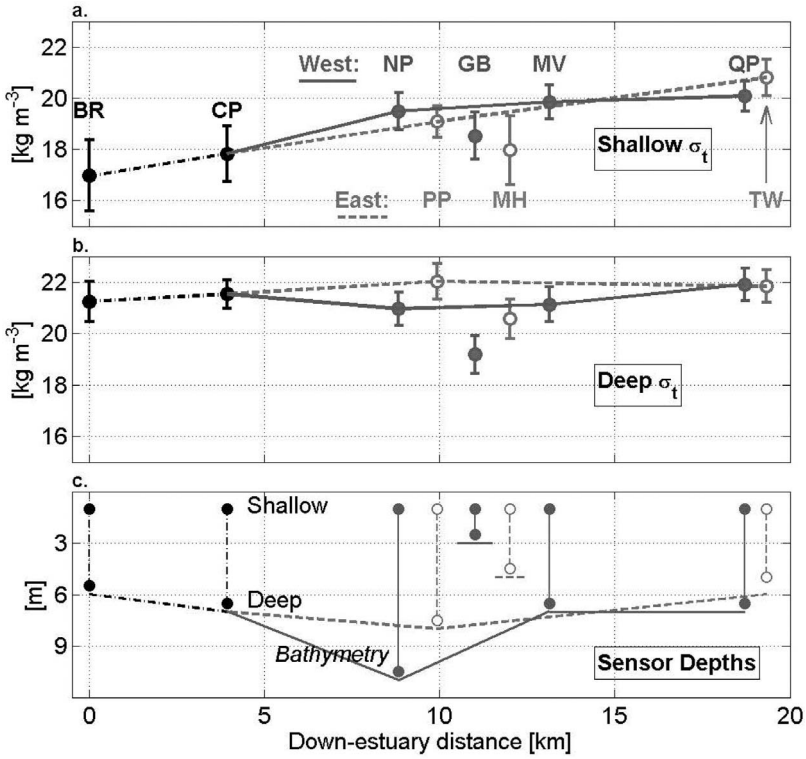

Figure 6. Down-estuary and east-west structure of density (sigma-t): multiyear average (curves) and interannual variability (error bars are standard deviation) of 5-month mean. (a) Near-surface sensors ("shallow") with stations labeled. (b) Near-seafloor sensors ("deep"). (c) Depths of sensors, and bathymetry. Horizontal axis is down-estuary distance toward the coastal ocean, as defined in the methods section. Northernmost stations (BR and CP) are shown using black solid symbols connected by dash-dot lines. Stations extending southward along the west (NP, MV, and QP) are shown using darker gray solid symbols with connecting solid lines; the western embayment station (GB), shown separately, has the same symbol/shade. Stations extending southward along the east (PP, TW) are shown using lighter gray open symbols with connecting dashed lines; the eastern embayment station (MH), shown separately, has the same symbol/shade.

[27] Salinities (Figure 4) at shallow and deep depths follow distinctly different seasonal progressions from each other. Shallow salinities mirror river flow (Figure 2) with minima (down to 23 PSS at BR) in spring and summer (MJ, JJ, and JA, with JJ typically the freshest) with higher values (about 27–30 PSS) in late summer and fall (AS and SO, with SO slightly fresher); the northern and central sites see far fresher salinities due to their proximity to river inputs (Figure 2). Deep salinities are relatively uniform bay-wide and remain effectively constant (near 30 PSS) or increase weakly (by 1–2 PSS) from spring through summer and early fall. Vertical salinity differences therefore mostly reflect shallow salinity variability: they are largest toward the north and east (at BR, CP, PP and MH) and weakest at GB; maxima reach about 7 PSS during early and mid-spring (MJ, JJ) and minima of 1–2 PSS occur in AS or SO.

[28] Densities (Figure 5) are influenced most strongly by salinity at northern and central sites, with spring minima of about 15 kg m^{-3} and maxima of roughly 19–22 kg m^{-3} later in the year. Though generally a secondary influence, vertical temperature differences cause the density minima to occur later in the spring than the minima in salinity. At southern sites, the seasonal progression of shallow densities has a modest overall range of about 2–3 kg m^{-3} and primarily follows the influence of temperature, with a late summer minimum between higher values in spring and fall. The seasonal progression of deep densities is similar at all stations, as influenced by deep temperatures because deep salinities vary little seasonally.

[29] Stratification (deep minus shallow density) is strongest in northern and eastern parts of the bay, including the MH embayment, with maxima in early or mid-spring at about 4–7 kg m^{-3} and minima of about 2–3 kg m^{-3} in late summer and early fall. In southern areas stratification peaks at about 2–3 kg m^{-3} in spring and falls off to 1–2 kg m^{-3} in summer and fall. The salinity contribution to vertical density differences (Figure 5) is typically 70–90%, with smallest values (50–60%) mainly at southern stations from about late spring to early summer, during peak vertical temperature differences. In early fall (SO), salinity drives more than 85% of vertical density differences at all stations and more than 95% at most.

3.3. Horizontal Density Structure

[30] A vertical-slice depiction (Figure 6) of down-estuary and east-west structure of density, using the 5-month means, complements the above descriptions. Along both the eastern and western sides of the bay, excluding the embayment stations, the shallow densities (Figure 6, top) are characterized

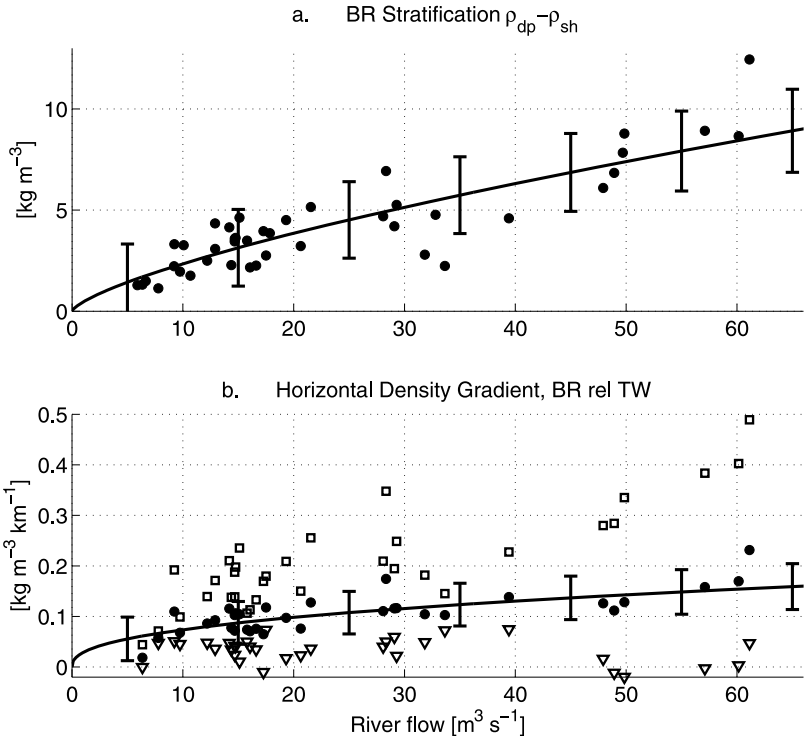

Figure 7. (a) Individual points: Monthly mean stratification at BR as a function of monthly mean river flow (Table 5, first row). Curve and bars: Best fit power law model with 90% confidence level in model fit. (b) Solid circles, curve, and bars: Horizontal gradient of vertical-mean density (shallow and deep measurements weighted by layer thicknesses) between BR and TW stations, as function of monthly mean river flow, with power law model results (Table 6, third row), presented as in Figure 7a. Open squares and triangles show gradients based on shallow and deep measurements, respectively, instead of layer-weighted vertical mean.

by a generally uniform down-estuary increase of about 4 kg m^{-3} (from 17 to 21 kg m^{-3}) over about 20 km, corresponding to a gradient of about 0.2 kg m^{-3} km^{-1}. The deep densities (Figure 6, middle) are more uniform bay-wide, with an overall down-estuary increase of less than 1 kg m^{-3} over 20 km. East-west structure in density is not pronounced, excluding embayment stations. However, there is weak evidence that near down-estuary distances of about 7 to 14 km (stations NP, PP, and MV) deep densities are higher in the east (by up to 1 kg m^{-3}), and shallow densities are higher in the west by a similar amount. For the embayment stations, GB and MH, at both the shallow and deep depths the densities are lower than other stations near to them. In GB it is the deep sensor that has the markedly lower density compared to deep densities at other stations, as expected in association with how shallow the site is. In contrast to GB where there is no river input, at MH the lower densities are due to proximity to the Taunton River.

3.4. Inter-annual Variability and Its Relation to Driving Factors

[31] Inter-annual variability in stratification (Figure 5, error bars) is typified by standard deviations of individual monthly mean values that are about half the mean values. The dominant contribution is inter-annual variability in vertical salinity differences (Figure 4, error bars). Nine-year time series showing the 5-month means of each individual year (Figure 7) reveal important characteristics of the nature of inter-annual variability in density and density stratification. The most prominent feature is individual years (for example, 2001, 2003, 2006, and to some extent 2009) during which surface density is significantly lower, and hence stratification more pronounced. During these years similar increases in stratification occur at all stations; to further quantify the extent of the geographic uniformity in the response, deviations of individual monthly means from the multiyear mean for that month are used. Kendall's τ correlations (Table 5) between every station pair were significant (the maximum p value was 0.034;

Table 5. Results of k and α Values From Best Fit of Observed Monthly Mean Stratification (Number of Data *n*) to Power Law kQ^{α} Function of Monthly Mean River Flow Q (m^3 s^{-1})[a]

Station (See Figure 1)	n	k	α	90% Conf. Int. on α
BR	42	0.46	0.71	0.11
CP	27	0.46	0.64	0.12
NP	39	0.18	0.64	0.15
MV	26	0.13	0.65	0.22
QP	19	0.34	0.45	0.18
PP	25	0.62	0.45	0.11
TW	35	0.11	0.67	0.18
GB	32	0.06	0.73	0.23
MH	21	0.44	0.71	0.12

[a]For all stations except MH, Q is the summed flow from the Blackstone, Pawtuxet, Ten Mile, Woonasquatucket, and Moshassuck Rivers, and for the MH station Q is the flow from the Taunton River.

n ranges from 18 to 37 out of 45 maximum possible for 5 monthly intervals in 9 years), with all τ values positive and in the range from 0.357 to 0.705.

[32] Visual comparisons of the inter-annual variability of the 5-month mean stratification to that of the driving factors (river flow, heat flux, wind speed) averaged over the same 5 months (Figure 8, top right frames) are instructive. Years with higher than average river flow have higher than average stratification, particularly in 3 of the 4 most strongly stratified years (2003, 2006, and 2009). In contrast, the inter-annual variability in heat flux and wind speed shows little evident relationship with that of stratification. Prominent examples underscoring this are the anomalously low heat flux in 2009, and the anomalously high wind speed in 2006; each would be expected to weaken stratification, but stratification was nonetheless higher than average in both those years.

[33] These patterns are quantified by Kendall's τ correlation results. For river flow, correlations are significant at all sites (maximum p value of 0.007) with τ values all positive: 0.673, 0.727, 0.606 at BR, CP, and NP; 0.459 and 0.450 at MV and QP; 0.547 and 0.482 at PP and TW; and 0.452 and 0.600 at GB and MH.

[34] For heat flux, as expected given the minor influence of temperature on stratification, a pattern of strong correlations was not found. Correlation was significant only at MH, with $p = 0.0420$ and $\tau = -0.324$, which is considered spurious. Negative τ corresponds to negative stratification deviation for positive heat flux deviation, opposite the physical expectation. There is no plausible mechanism to explain this even if the potential role of the thermal discharge from a power plant, possibly important to the Mount Hope Bay heat budget [*Fan and Brown*, 2006; *Swanson et al.*, 2006], is invoked.

[35] No p value was significant for any wind parameter (speed, constancy, component along 16 compass directions) at any site.

[36] In summary, inter-annual variability in stratification is strongly dominated by inter-annual variability in river flow, with inter-annual variability in heat flux and wind parameters of secondary importance.

3.5. Response to River Forcing in Context of Theoretical Scaling

[37] The power law fit of stratification dependence on river flow (Table 5, all stations; Figure 7a shows BR as an example) yields exponents in the range of 0.45–0.73 and average value of 0.63 across all 9 stations. Despite substantial variability, as quantified by 90% confidence intervals on the exponent in the range 0.11–0.23, these results are in agreement with the 2/3 exponent of the theoretical scaling. With few exceptions, differences in the exponent from station to station are not significant, indicating that within uncertainties the response is generally geographically uniform.

[38] The power law fit of the river flow dependence of the horizontal gradient of the layer-weighted vertical-mean densities (Table 6; Figure 7b shows an example for the BR-TW station pair representing East Passage) yields exponents in the range 0.41–0.57. There is substantial variability, just as for stratification, with 90% confidence intervals on the exponent in the range 0.11–0.23. The confidence intervals marginally span a range that includes, near its lower end, the 1/3 exponent of the theoretical scaling. However, the shallow and deep horizontal gradients (squares and triangles in Figure 7b) are substantially stronger and weaker than the gradient of the layer-weighted vertical mean densities. Thus the exponent in the power law fit is sensitive to the nature of the layer-weighting in the calculation of the vertical-mean densities, and further conclusions are limited by the lack of detailed information about layer thicknesses.

3.6. Relationship Between Stratification and Hypoxia

[39] To assess the extent to which inter-annual variations in stratification and hypoxia are related, Kendall's τ was computed between the bay-wide seasonal hypoxia index and the stratification, similarly averaged over the available data from the same four stations used in the hypoxia index (BR, CP, NP, MV), in all available years ($n = 9$). The correlation with stratification during the late spring (MJ, May 15–Jun 15; Figure 8) is significant ($p = 0.0247$), moderately strong, and positive ($\tau = 0.611$). Correlations of bay-wide hypoxia index with the 5-month mean stratification, and with the stratification during monthlong periods other than MJ, were not significant. No correlations between the seasonal hypoxia index and stratification, both computed at an individual station (e.g., not bay-wide averages), were significant at any station, using individual months or the 5-month mean.

4. Discussion

[40] Observations of NB residual flow are sparse [*Spaulding and Swanson*, 2008] and the resulting poor understanding of circulation pathways and transport rates limits progress understanding mechanisms governing the density field in NB. Nonetheless key features of deep temperature and salinity fields described here are consistent with the importance of a persistent estuarine exchange flow in sustaining the observed stratification. Deep salinities that are relatively uniform in the along-passage direction, and that have a weak seasonal progression, are indicative that deep waters are continually replenished by northward flow of oceanic origin. They also suggest that exchange of water properties between deep and shallow layers is primarily occurring by entrainment, which modifies the deep layer weakly, in far northern areas.

4.1. Unexpectedly Uniform Geographic Structure and Response

[41] The fact that the density structures in the East and West Passages are so similar (Figures 5 and 6) is surprising considering their relative isolation from one another spatially together with the fact that order one or greater Kelvin number estimates imply importance of background rotation. Consider a bay as wide as NB but that is not divided in to passages by islands as is NB; scaling [e.g., *Valle-Levinson*, 2008] suggests an asymmetric structure of density-driven exchange flow due to the Coriolis force (such asymmetry is observed in other systems, for example LIS [*Codiga and Aurin*, 2007]) that could be expected to cause higher and lower densities in the East and West Passages, respectively. An asymmetry of this type, if present in NB (Figure 6), is weak and mainly occurs at depth. Inter-annual variability in stratification is also substantially geographically uniform (Table 5). A plausible explanation for the weak spatial structure in density and its inter-annual variability is that the complex geometry effectively causes it to behave as a narrow

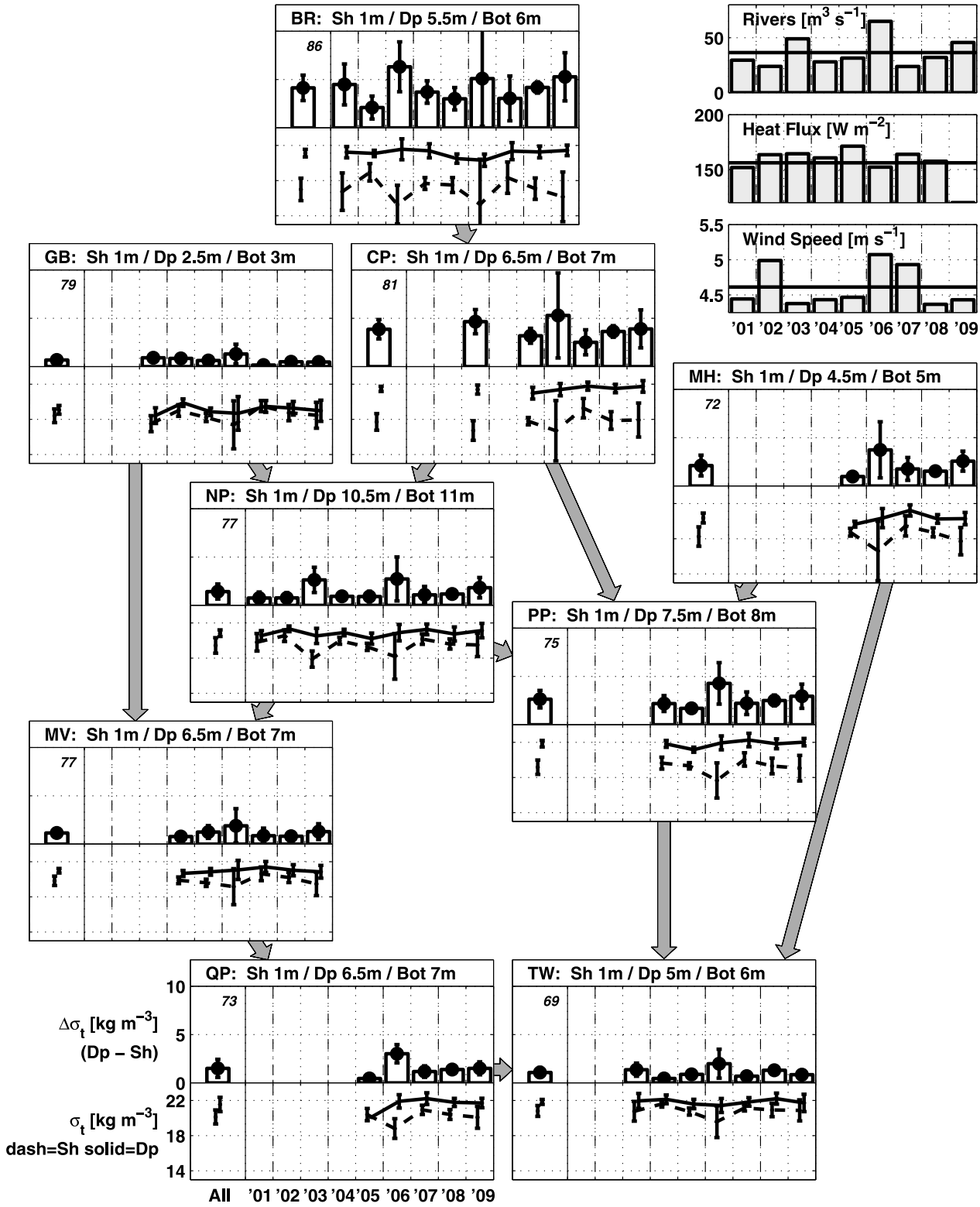

Figure 8. Inter-annual variability in density and vertical density difference. Top frames show vertical density difference and bottom frames show the shallow (dashed) and deep (solid) density, with small right-left offsets for clarity to avoid error bar overlap. Legends in bottom left frame. In the left portion of each frame are the multiyear means, using all available years, with error bars indicating the inter-annual variability (standard deviation of the annual-means); the number above the leftmost bar is the percent of the mean vertical density difference due to salinity. In the right plots of each frame are the 5-month means, with error bars indicating standard deviations of the 5 one-month means in that year. Upper right: 5-month mean river flow, heat flux, and wind speed, with 2001–2009 mean as horizontal line.

Table 6. Results of k and α Values From Best Fit of Observed Axial Gradient of Layer-Weighted Vertical Mean Density (Number of Data *n*) to Power Law kQ^{α} Function of Monthly Mean River Flow Q (Summed Flow From the Blackstone, Pawtuxet, Ten Mile, Woonasquatucket, and Moshassuck Rivers; $m^3\ s^{-1}$)

Station Pair	n	k	α	90% Conf. Int. on α
BR – NP	37	0.03	0.57	0.18
BR – QP	18	0.02	0.50	0.23
BR - TW	33	0.03	0.41	0.11

system (low Kelvin number), but further investigation of the dynamics is needed.

4.2. Comparison to Other Systems: Insensitivity to Wind

[42] The NB density field is most similar to CB [e.g., *Hagy et al.*, 2004], where salinity dominates and the seasonal progression does not involve a temperature-driven late summertime peak in stratification as in western LIS [e.g., *Kaputa and Olsen*, 2000]. This similarity between NB and CB extends to the fact that inter-annual variability in stratification is tied most closely to late spring river runoff [*Hagy et al.*, 2004].

[43] The insensitivity of NB stratification to inter-annual variability in wind-forcing sets it apart from CB and LIS. This is somewhat surprising because NB is shallower than these other systems. The most plausible explanation is that fetch is more limited in NB. The complex geometry, somewhat smaller overall breadth, and weaker alignment of the main passageways with prevailing winds are all likely contributing factors.

4.3. Response to River Forcing

[44] The power law fits (Figure 8) indicate NB stratification is marginally more reactive (larger exponent) than the axial gradient, to within uncertainties. This is qualitatively consistent with theoretical scaling for stratification and axial gradient as the 2/3 and 1/3 power of river flow respectively [e.g., *Hetland and Geyer*, 2004; *MacCready and Geyer*, 2010]. The NB stratification response agrees well quantitatively with the 2/3 exponent.

[45] Results for the response of the axial gradient are less conclusive but nonetheless indicate it responds at least as strongly as the 1/3 exponent. This suggests NB differs from other systems in which axial gradients, based on the instrusion length, are very weakly responsive to river flow (e.g., Delaware Bay [*Garvine et al.*, 1992]; and SF Bay [*Monismith et al.*, 2002] where a 1/7 exponent applies).

[46] Agreement of the observed stratification response with the 2/3 exponent scaling is surprising in the sense that the theory has been developed for an idealized system that does not include key features of NB. One such feature is that the horizontal density gradients vary more strongly with depth than the structure presumed by the theory. NB is partially stratified, and far from the salt-wedge limit, but nonetheless has a distinct two-layer structure with weak gradients in the deep layer (Figure 6). Another important attribute of NB is that the estuary length, the distance between its oceanic endpoint and freshwater limit, is not free to adjust as in the theory. Instead the northern extent of the estuary is set by Pawtucket Falls (about 1 km north from the top edge of Figure 1, where Blackstone River waters enter bay water of salinity about 20 PSS), which acts as a barrier to further landward penetration of the salt intrusion. It is plausible that this attribute of NB plays a role in its higher responsiveness of horizontal gradients to river flow, as compared to theory and other estuaries. Generalizing the theory to accommodate vertically varying horizontal density gradients, and basin-size constrained estuary lengths, would make it more applicable to estuaries with these features, such as NB.

4.4. Relationship Between Stratification and Hypoxia

[47] The finding that inter-annual variations in the bay-wide seasonal hypoxia index correlate moderately strongly with late spring (MJ) stratification (Figure 9), but not the 5-month mean stratification, underscores that the influence of stratification on seasonal-mean hypoxia involves a lag time

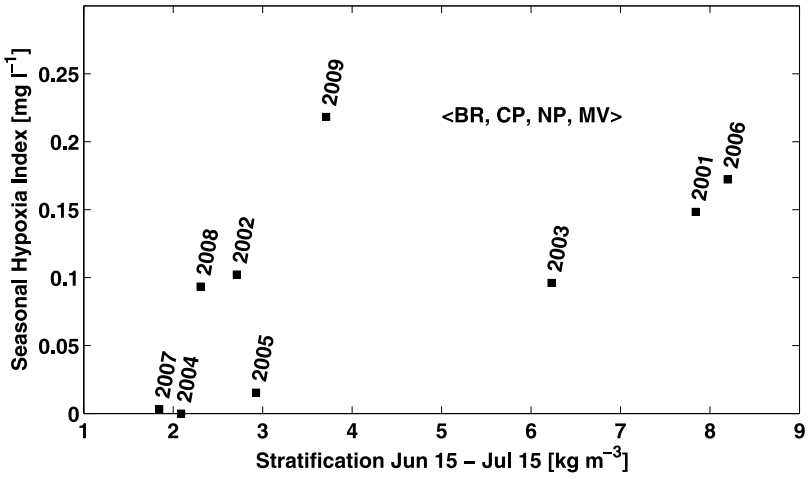

Figure 9. Inter-annual variations in the seasonal hypoxia index and the late spring (Jun 15 to Jul 15 mean) stratification. The seasonal hypoxia index is the season-cumulative deficit-duration (relative to 2.9 mg l^{-1}, for trigger duration 9 h and minimum event duration 1 day), normalized by the days sampled that season, and averaged across BR, CP, NP, and MV stations. Stratification is averaged over the same stations.

Table 7. Station to Station Correlations of Inter-annual Deviations of Stratification[a]

	CP	NP	MV	QP	PP	TW	GB	MH
BR	0.705	0.646	0.473	0.438	0.558	0.428	0.402	0.463
CP		0.567	0.573	0.462	0.550	0.618	0.595	0.552
NP			0.563	0.591	0.693	0.492	0.454	0.667
MV				0.380	0.567	0.403	0.508	0.486
QP					0.626	0.357	0.520	0.477
PP						0.500	0.493	0.590
TW							0.375	0.400
GB								0.457

[a]Kendall's Tau for deviations of monthly mean (MJ, JJ, JA, AO, SO) stratification relative to multiyear means over the corresponding monthly intervals; all p values are <0.035 and *n* ranges from 18 to 37 (max possible 45, for 5 monthly intervals in 9 years).

of up to a few months. Similar results from earlier analysis, using shorter time series and fewer stations [*Codiga et al.*, 2009], are therefore applicable at a larger spatial scales.

[48] The geographic structure of stratification consists of peak values toward the north and east (Figure 5). In contrast, the geographic structure of hypoxia has peak values in the north and west [*Codiga et al.*, 2009], due to the combined influences of a north-south gradient in nutrient load and productivity, and the east-west structure of the residual flow.

[49] In addition to their partial overlap spatially, inter-annual variability (Figure 9) underscores that that the one-dimensional paradigm for stratification driving hypoxia by suppressing vertical mixing locally is not particularly applicable. While 3 of the 4 most strongly stratified years (2001, 2006, 2009) correspond to the 3 highest hypoxia index values, the year with 3rd highest stratification (2003) had hypoxia index equivalent to that during two years when stratification was weaker than average (2002, 2008). So although stratification has been shown to be the parameter most closely tied to hypoxia among a wide array of available biological and physical measurements [*Codiga et al.*, 2009], there is a limit to the strength of the relationship. Furthermore, the lack of significant correlations between seasonal hypoxia index and stratification when both are computed at individual stations suggests that local advection, which is not part of the one-dimensional paradigm but for which observations are the most limited, is important.

4.5. Implications for Response to Climate Change

[50] Climate change trends for NB are documented. River flow increased by ~13% over the past 40 years and precipitation increased by ~30% over the past 100 years [*Pilson*, 2008]. Water temperatures have increased by 1–2 C over the past several decades [*Oviatt*, 2004]. Monthly mean wind speeds appear to have decreased by significant fractions over the past 50 years [*Pilson*, 2008]. Regional forecasts suggest precipitation and temperatures will continue to increase [*Frumhoff et al.*, 2007].

[51] The NBFSMN observations used, with the longest records (at just 2 of the 9 sites) of 8–9 years and strong inter-annual variability, do not yet support investigation of long-term trends. However, to the extent the present findings about inter-annual variability are relevant to long-term trends, they suggest that climate-driven changes in NB stratification will be responsive mainly to changes in river runoff. Warming will play a minor role because, according to the seawater equation of state, a 1 kg m^{-3} density change requires a change of ~5 C in temperature or ~1 PSS in salinity. Density changes due to the 1–2 C warming over the past several decades thus have an upper bound (assuming the surface warms and deep water does not) of 0.1–0.2 kg m^{-3}; based on the observed 2/3 power law response (see above) the 13% increase to river flow over the past 40 years corresponds to an increase in stratification of 8.5%, or about 0.5 kg m^{-3} for a northern site with typical stratification of 6 kg m^{-3}. Insensitivity of inter-annual variability in NB to winds (see above) suggests wind will also be a minor influence on long-term trends. *Nixon et al.* [2009] emphasized that observed wind speed decreases in the last ~50 years correspond to a 45% decline in vertical mixing potential, but this is based on open-ocean wind mixing dynamics [*Niiler and Kraus*, 1977] that may not apply in estuaries.

5. Summary and Conclusions

[52] Monthly means computed from 4 to 9 years of high temporal resolution time series, from late spring through fall at nine sites (Figure 1) spanning the northern portions of NB, were used to characterize the structure (Figure 6), seasonal progression (Figures 3–5) and inter-annual variability (Figure 7) of the density field including stratification and horizontal gradients. Relationships to river, heat flux, and wind-forcing (Figures 2, 7, and 8), and hypoxia (Figure 9) have been examined.

[53] Stratification (Figure 5) is influenced dominantly by salinity (typically responsible for 70–95% of vertical density difference), hence strongest in the north and east where river sources influence shallow values, and peaks in early spring followed by decreases through summer to fall. Horizontal structure of density (Figure 6) reveals a relatively uniform deep layer, in contrast to a shallow layer that is characterized by a nearly constant gradient of about 0.2 kg m^{-3} km^{-1} in the along-passage direction throughout the sampled area.

[54] Contrary to expectations, based on its complex geometry and scaling that indicates the importance of rotation given its breadth, in NB the large-scale geographic structure in the density field is not pronounced and differences between its two main passages are small. Geographic variability of inter-annual stratification anomalies (Figure 8) is also minor, with significant correlations among all station pairs (Table 7).

[55] Inter-annual changes in stratification at all sites correlate strongly with inter-annual river flow changes, but no correlations with inter-annual variations in heat flux, wind speed, wind constancy, or wind components from 16 compass directions are significant. Insensitivity to wind-forcing sets NB apart from other systems nearby (CB and LIS). It is likely due to limited fetch associated with its more complex geometry, narrower passages, and different orientation relative to the prevailing wind direction.

[56] The response of NB stratification to river forcing agrees (Table 5) with a theoretical 2/3 power law, which is surprising given that the idealized system to which the theory applies omits key characteristics of NB (e.g., complex geometry, influence of rotation, horizontal density gradients that vary with depth). The non-uniform vertical structure of horizontal density gradients in NB complicates comparing their response to river forcing against theoretical scaling. However, results suggest horizontal gradients are at least as

responsive to river forcing as the theoretical 1/3 power law (Table 6), which sets NB apart from other apparently less-responsive systems (e.g., Delaware Bay, SF Bay), and may be associated with a falls near the head of NB that impedes free adjustment of the intrusion length.

[57] The geographic structure of stratification (strongest in the north and east) overlaps partially with that of hypoxia (strongest in the north and west). At the bay-wide scale, inter-annual variations in late spring stratification correlate significantly with those of seasonal hypoxia (Figure 9). However, correlations between stratification and hypoxia at individual stations are not significant. The relationship is more complex than the one-dimensional (vertical) paradigm for hypoxia resulting from stratification suppressing mixing, suggesting the importance of advection.

[58] Based on the inter-annual variability observed and known long-term trends, response of density and stratification in NB to climate change will be dominated by increasing river flow rather than increasing temperatures.

[59] **Acknowledgments.** Heather Stoffel is thanked for promptly sharing NBFSMN files as she completed their quality control and processing. The analysis was only possible due to sustained sampling by the NBFSMN, as carried out collectively by several institutions: the Water Resources Division of the RI Department of Environmental Management, the Narragansett Bay National Estuarine Research Reserve, the Narragansett Bay Commission, and URI/GSO. Funded by the NOAA Coastal Hypoxia Research Program (CHRP), grant NA05NOS4781201, CHRP contribution number 169.

References

Altieri, A., and J. Witman (2006), Local extinction of a foundation species in a hypoxic estuary: Integrating individuals to ecosystem, *Ecology*, *87*, 717–730, doi:10.1890/05-0226.

Asselin, S., and M. L. Spaulding (1993), Flushing times for the Providence River based on tracer experiments, *Estuaries*, *16*(4), 830–839, doi:10.2307/1352442.

Bates, D. M., and D. G. Watts (Eds.) (1988), *Nonlinear Regression Analysis and its Applications*, John Wiley, New York, doi:10.1002/9780470316757.

Bergondo, D. L. (2004), Examining the processes controlling water column variability in Narragansett Bay: Time series data and numerical modeling, doctoral dissertation, 136 pp., Grad. School of Oceanogr., Univ. of R. I., Narragansett.

Bergondo, D. L., D. R. Kester, H. E. Stoffel, and W. L. Woods (2005), Time-series observations during the low sub-surface oxygen events in Narragansett Bay during summer 2001, *Mar. Chem.*, *97*(1–2), 90–103, doi:10.1016/j.marchem.2005.01.006.

Berman, M. S. (2008), Narragansett Bay Monthly Transect, http://www.narrbay.org/d_projects/nushuttle/shuttletree.htm, Natl Mar. Fish. Serv., Narragansett, R. I.

Codiga, D. L. (2008), A moving window trigger algorithm to identify and characterize hypoxic events using time series observations, with application to Narragansett Bay, *GSO Tech. Rep. 2008-01*, 110 pp., Univ. of R. I., Narragansett. [Available at ftp://po.gso.uri.edu/pub/downloads/codiga/chrp/mwt/TechRptMWTCodigaMar08.pdf.]

Codiga, D. L., and D. A. Aurin (2007), Residual circulation in eastern Long Island Sound: Observed transverse-vertical structure and exchange transport, *Cont. Shelf Res.*, *27*, 103–116, doi:10.1016/j.csr.2006.09.001.

Codiga, D. L., H. E. Stoffel, C. F. Deacutis, S. Kiernan, and C. Oviatt (2009), Narragansett Bay hypoxic event characteristics based on fixed-site monitoring network time series: Intermittency, geographic distribution, spatial synchronicity, and inter-annual variability, *Estuaries Coasts*, *32*(4), 621.

Deacutis, C. F. (2008), Evidence of ecological impacts from excess nutrients in Upper Narragansett Bay, in *Science for Ecosystem-Based Management: Narragansett Bay in the 21st Century*, *Springer Ser. Environ. Manage.*, edited by A. Desbonnet and B. A. Costa-Pierce, pp. 349–381, Springer, New York, doi:10.1007/978-0-387-35299-2_12.

Deacutis, C. F., D. W. Murray, W. L. Prell, E. Saarman, and L. Korhun (2006), Hypoxia in the upper half of Narragansett Bay, RI, during August 2001 and 2002, *Northeast. Nat.*, *13*(4), 173–198, doi:10.1656/1092-6194(2006)13[173:HITUHO]2.0.CO;2.

Fan, Y., and W. S. Brown (2006), On the heat budget for Mount Hope Bay, *Northeast. Nat.*, *13*, 47–70, doi:10.1656/1092-6194(2006)13[47:OTHBFM]2.0.CO;2.

Fish, C. J. (Ed.) (1953), Physical oceanography of Narragansett Bay - Rhode Island Sound, I.S.P. final report, Univ. of R. I., Kingston.

Frumhoff, P., J. McCarthy, J. Melillo, S. Moser, and D. Wuebbles (2007), Confronting climate change in the U.S. Northeast: Science, impacts, and solutions, synthesis report of the Northeast Climate Impacts Assessment, 160 pp., Union of Concerned Sci., Cambridge, Mass.

Garvine, R. W. (1995), A dynamical system for classifying buoyant coastal discharges, *Cont. Shelf Res.*, *15*(13), 1585–1596, doi:10.1016/0278-4343(94)00065-U.

Garvine, R. W., R. K. McCarthy, and K. C. Wong (1992), The axial salinity distribution in the Delaware estuary and its weak response to river discharge, *Estuarine Coastal Shelf Sci.*, *35*, 157–165, doi:10.1016/S0272-7714(05)80110-6.

Hagy, J. D., W. R. Boynton, C. W. Keefe, and K. V. Wood (2004), Hypoxia in Chesapeake Bay, 1950–2001: Long-term change in relation to nutrient loading and river flow, *Estuaries*, *27*, 634–658, doi:10.1007/BF02907650.

Hetland, R., and W. R. Geyer (2004), An idealized study of the structure of long, partially mixed estuaries, *J. Phys. Oceanogr.*, *34*, 2677–2691, doi:10.1175/JPO2646.1.

Hicks, S. D. (1959), The physical oceanography of Narragansett Bay, *Limnol. Oceanogr.*, *4*, 316–327, doi:10.4319/lo.1959.4.3.0316.

Kaputa, N. P., and C. B. Olsen (2000), Summer Hypoxia Monitoring Survey '91–'98 Data Review, report, State of Conn. Dep. of Environ. Protect., Hartford.

Kremer, J. N., and S. Nixon (1978), *A Coastal Marine Ecosystem, Simulation and Analysis*, *Ecol. Stud.*, *24*, 217 pp.

MacCready, P., and W. R. Geyer (2010), Advances in estuarine physics, *Annu. Rev. Mar. Sci.*, *2*, 35–58, doi:10.1146/annurev-marine-120308-081015.

Melrose, D. C., C. A. Oviatt, and M. S. Berman (2007), Hypoxic events in Narragansett Bay, Rhode Island, during the summer of 2001, *Estuaries Coasts*, *30*(1), 47–53.

Mesinger, F., et al. (2006), North American Regional Reanalysis, *Bull. Am. Meteorol. Soc.*, *87*(3), 343–360, doi:10.1175/BAMS-87-3-343.

Monismith, S. G., W. Kimmerer, J. R. Burau, and M. T. Stacey (2002), Structure and flow-induced variability of the subtidal salinity field in northern San Francisco Bay, *J. Phys. Oceanogr.*, *32*(11), 3003–3019, doi:10.1175/1520-0485(2002)032<3003:SAFIVO>2.0.CO;2.

Narragansett Bay Fixed-Site Monitoring Network (NBFSMN) (2004), 2004 datasets, www.dem.ri.gov/bart, R. I. Dep. of Environ. Manage., Providence.

Narragansett Bay Fixed-Site Monitoring Network (NBFSMN) (2005), 2005 datasets, www.dem.ri.gov/bart, R. I. Dep. of Environ. Manage., Providence.

Narragansett Bay Fixed-Site Monitoring Network (NBFSMN) (2006), 2006 datasets, www.dem.ri.gov/bart, R. I. Dep. of Environ. Manage., Providence.

Narragansett Bay Fixed-Site Monitoring Network (NBFSMN) (2007a), Narragansett Bay Fixed Site Monitoring Network, http://www.dem.ri.gov/bart/stations.htm, R. I. Dep. of Environ. Manage., Providence.

Narragansett Bay Fixed-Site Monitoring Network (NBFSMN) (2007b), 2007 datasets, www.dem.ri.gov/bart, R. I. Dep. of Environ. Manage., Providence.

Narragansett Bay Fixed-Site Monitoring Network (NBFSMN) (2008), 2008 datasets, www.dem.ri.gov/bart, R. I. Dep. of Environ. Manage., Providence.

Narragansett Bay Fixed-Site Monitoring Network (NBFSMN) (2009), 2009 datasets, www.dem.ri.gov/bart, R. I. Dep. of Environ. Manage., Providence.

Niiler, P. P., and E. B. Kraus (1977), One dimensional models of the upper ocean, in *Modeling and Prediction of the Upper Layers of the Ocean*, edited by E. B. Kraus, 143–172, Permagon, New York.

Nixon, S., R. W. Fulweiler, B. A. Buckley, S. Granger, B. L. Nowicki, and K. M. Henry (2009), The impact of changing climate on phenology, productivity, and benthic-pelagic coupling in Narragansett Bay, *Estuarine Coastal Shelf Sci.*, *82*, 1–18, doi:10.1016/j.ecss.2008.12.016.

Oviatt, C. A. (2004), The changing ecology of temperate coastal waters during a warming trend, *Estuaries*, *27*(6), 895–904, doi:10.1007/BF02803416.

Pilson, M. E. Q. (1985), On the residence time of water in Narragansett Bay, *Estuaries*, *8*, 2–14, doi:10.2307/1352116.

Pilson, M. E. Q. (2008), Narragansett Bay amidst a globally changing climate, in *Science for Ecosystem-Based Management: Narragansett Bay in the 21st Century*, *Springer Ser. Environ. Manage.*, edited by A. Desbonnet and B. A. Costa-Pierce, pp. 35–46, Springer, New York, doi:10.1007/978-0-387-35299-2_2.

Rhode Island Department of Environmental Management (RIDEM) (2005), Plan for managing nutrient loadings to Rhode Island waters, report, 17 pp., Providence. [Available at http://www.dem.ri.gov/pubs/nutrient.pdf.]

Rhode Island Department of Environmental Management (RIDEM) (2007), Quality assurance project plan: Narragansett Bay fixed-site water quality monitoring network seasonal monitoring, report, 37 pp., Providence. [Available at http://www.dem.ri.gov/pubs/data.htm#quapps.]

Ries, K. G. (1990), Estimating surface-water runoff to Narragansett Bay, Rhode Island and Massachusetts, *U. S. Geol. Surv., Water-Resour. Invest. Rep.*, *89-4164*, 1–49.

Rogers, J. M. (2008), Circulation and transport in the heart of Narragansett Bay, M.S. thesis, 95 pp., Grad. School of Oceanogr., Univ. of R. I., Narragansett.

Scully, M. E. (2010), Wind modulation of dissolved oxygen in Chesapeake Bay, *Estuaries Coasts*, *33* 1164–1175, doi:10.1007/s12237-010-9319-9.

Seber, G. A. F., and C. J. Wild (2003), *Nonlinear Regression*, Wiley-Interscience, Hoboken, N. J.

Spaulding, M. L., and R. L. Swanson (2008), Circulation and transport dynamics in Narragansett Bay, in *Science for Ecosystem-Based Management: Narragansett Bay in the 21st Century*, *Springer Ser. Environ. Manage.*, edited by A. Desbonnet and B. A. Costa-Pierce, pp. 233–279, New York, doi:10.1007/978-0-387-35299-2_8.

Stoffel, H. E. (2003), Corrected data sets, NBFSMN 2003, report, Univ. of R. I., Narragansett. [Available at www.narrbay.org.]

Swanson, C., H. S. Kim, and S. Sankaranarayanan (2006), Modeling of temperature distributions in Mount Hope Bay due to thermal discharges from the Brayton Point Station, *Northeast. Nat.*, *13*, 145–172, doi:10.1656/1092-6194(2006)13[145:MOTDIM]2.0.CO;2.

Valle-Levinson, A. (2008), Density-driven exchange flow in terms of the Kelvin and Ekman numbers, *J. Geophys. Res.*, *113*, C04001, doi:10.1029/2007JC004144.

Weisberg, R. H., and W. Sturges (1976), Velocity observations in the West Passage of Narragansett Bay: A partially mixed estuary, *J. Phys. Oceanogr.*, *6*, 345–354, doi:10.1175/1520-0485(1976)006<0345:VOITWP>2.0.CO;2.

Wilson, R. E., R. L. Swanson, and H. A. Crowley (2008), Perspectives on long-term variations in hypoxic conditions in western Long Island Sound, *J. Geophys. Res.*, *113*, C12011, doi:10.1029/2007JC004693.